Fast Communications

Time-resolved measurements of supersonic fuel sprays using synchrotron X-rays

Christopher F. Powell,[a] Yong Yue,[b] Ramesh Poola[b] and Jin Wang[a]*

[a]*Advanced Photon Source, Argonne National Laboratory, Argonne, IL 60439, USA, and* [b]*Energy Systems Division, Argonne National Laboratory, Argonne, IL 60439, USA. E-mail: wangj@aps.anl.gov*

A time-resolved radiographic technique has been developed for probing the fuel distribution close to the nozzle of a high-pressure single-hole diesel injector. The measurement was made using X-ray absorption of monochromatic synchrotron-generated radiation, allowing quantitative determination of the fuel distribution in this optically impenetrable region with a time resolution of better than 1 µs. These quantitative measurements constitute the most detailed near-nozzle study of a fuel spray to date.

1. Introduction

The detailed analysis of fuel sprays in combustion systems is recognized as a key to increasing combustion efficiency and reducing pollutant emission, in particular from diesel engines. An understanding of the liquid breakup mechanism in the region close to the nozzle has significant bearing on the design of nozzle geometry and is a key to realistic computational modeling. These interests have spurred considerable activity in the development of optical techniques (primarily using lasers) for measurements of diesel fuel injection systems (Hiroyasu, 1991; Maly *et al.*, 1991; Adrian, 1991; Shimizu *et al.*, 1982; Yeh *et al.*, 1993; Coil & Farrell, 1995; Long *et al.*, 1996). Some of these optical techniques have become commercially available and can be readily applied to the testing and development of modern injection systems.

Despite significant advances in laser diagnostics over the last 20 years, multiple scattering from the large number of droplets prevents the penetration of the light in the near-nozzle region and limits quantitative evaluation with optical techniques. While other researchers are looking into the possibility of using lasers of ultrahigh power and ultrashort pulses to probe the near-nozzle region, we report here the development of a new nonintrusive, quantitative, and highly time-resolved technique to characterize the dense part of the fuel spray using X-ray absorption techniques.

X-rays are highly penetrative in materials composed of extremely dense droplets composed of low-Z materials due to the intrinsically low interaction cross section. This makes X-rays a useful tool for spray studies designed to overcome the limitations of visible light. Previously, Woodward *et al.* (1995) used X-ray tube sources to perform radiographic studies of the liquid core structure of coaxial jets of high-Z materials on a relatively large scale (nozzle diameter ~5 mm). However, when an energy-dispersive X-ray beam is used as the radiographic light source, as was the case in this radiographic experiment, a quantitative analysis of the absorption is extremely difficult. Therefore, a quantitative study of sprays must utilize a monochromatic X-ray beam.

For single-wavelength X-rays transmitting through an attenuating material, the analysis of the radiographic image of the attenuating material is straightforward and follows the form

$$I/I_0 = \exp(-\mu_M M), \tag{1}$$

where I and I_0 are the transmitted and incident beam intensities, respectively, μ_M is the mass absorption coefficient, and M is the total mass in the beam. Since μ_M can be measured accurately for the absorbing medium at a single wavelength, the amount of fuel in the beam path can be easily deduced from the transmission, I/I_0. Parenthetically, we note that in order to use equation (1) for calibration, the size of the X-ray beam should be the same for both measurement and calibration.

With the advent of third-generation synchrotron sources, extremely brilliant monochromatic X-ray beams are now available. These sources have paved the way for fast experiments of this type using monochromatic beams and achieving time resolution of 1 µs or better. For example, at the Advanced Photon Source (APS) bending-magnet beamlines, the high-energy storage ring produces brilliant wide-band X-ray beams of the order of 10^{17} photons s^{-1}. Even with high monochromaticity (*e.g.* 1.5×10^{-4} bandwidth), one can obtain ~10^{12} photons s^{-1} focused to a 0.6 mm × 0.3 mm beam spot (Lang *et al.*, 1999). In this paper, we report the first attempt to use these powerful yet nonintrusive beams to study fuel sprays from a high-pressure diesel injector.

2. Experimental setup

A high-pressure injection system similar to that of a passenger car with a specially fabricated single-orifice nozzle was employed. Injection was performed into a spray chamber with flowing inert gas at atmospheric pressure and ~298 K. The spray chamber was used to hold the injector, contain the spray plume, and allow the inert gas to scavenge the fuel vapors. The spray chamber has 50 mm-long and 25 mm-wide windows that provide line-of-sight access for the X-rays. Two different gases were used in the spray chamber: sulfur hexafluoride (SF$_6$) and nitrogen (N$_2$). SF$_6$, which is a very heavy gas (molecular weight of 146), was used to simulate the relatively dense ambient environment inside an automotive diesel engine. We note that the speed of sound in SF$_6$ is much less than in N$_2$ and is estimated to be ~140 m s^{-1}. The fuel used in this study was a blend of Amoco No. 2 diesel and a cerium-containing additive with a final cerium concentration of ~4% by weight. The cerium additive is a critical component of this study, as it accounts for more than 50% of the total X-ray absorption at the X-ray energy used in these measurements. The additive is a commercial product designed for diesel fuel systems and its effect on the spray structure is expected to be minimal since the density and viscosity of the blended fuel fall within the normal range for commercial diesel fuel.

The experiments were performed at bending-magnet beamline 1-BM of the SRI-CAT at the APS. The X-ray beam passed through a sagittal-focusing double-crystal monochromator tuned to a photon energy of 5.989 keV. This X-ray energy is just above the cerium L absorption edges near 5.7 keV (Henke *et al.*, 1993).

At its focal point in the 1-BM-C experimental radiation enclosure, the beam size was measured to be approximately 0.5 mm horizontally by 0.3 mm vertically (full width at half-maximum).

A schematic of the X-ray absorption setup for studying diesel sprays is shown in Fig. 1. The focused X-ray beam in the 1-BM-C station was defined by a pair of X-Y slits to a size of 500 µm (horizontal) $\times$ 50 µm (vertical). The beam intensity was monitored by an N_2 gas-filled ionization chamber. The collimated beam then passed into the injection chamber for probing the fuel sprays. To facilitate the alignment of the injector and the X-ray beam, another ionization chamber was positioned after the injection chamber.

The transient X-ray transmission signal due to the fuel spray was measured by an avalanche photodiode (APD). The APD has a fast response with temporal resolution of approximately 5 ns. The APD signal output was digitized by a 1 GHz oscilloscope (Tektronix TDS 784D) and recorded every 2 ns. Since the APD is a point detector, mapping the absorption (attenuation) image of the fuel spray involved translating the injection chamber vertically and horizontally with respect to the X-ray beam with micrometer resolution. This allowed the beam to probe various axial and radial positions within the spray plume.

The fuel injector was fired at a rate of 1 Hz, and an electronic gate with a width of 3.68 µs was generated from each fuel-injection event. The coincidence of this injection signal with the timing signal of the synchrotron was used as the trigger to the data acquisition. This timing setup ensured that the data acquisition was synchronized with the synchrotron X-ray pulses within 1 ns and synchronized with the fuel sprays with a jitter of a few microseconds. This allowed the results from successive sprays to be averaged, maximizing the signal-to-noise ratio.

Absorption measurements were performed while varying several different fuel spray parameters: injection pressure, injection duration, and ambient fill gas composition. For each set of spray parameters, absorption measurements were made at as many as 900 different axial and radial positions in a range from 0.5 to 40 mm from the nozzle. At each position, the results of 100 successive sprays were averaged in order to decrease the statistical uncertainty of the measurement. Here we present only those measurements made at an injection pressure of 500 bar and a duration of 300 µs in SF_6 ambient gas.

In order to understand the mechanics of the entire spray process, we attempted to capture the entire spray sequence, from before the opening of the injector solenoid, through the spray process, and after the spray had passed through the beam. For this reason we recorded the response of the APD for a time span of 1 ms for sprays of 300 µs duration.

The X-ray absorption technique using a monochromatic beam is distinguished from previous measurements of sprays by the quantitative nature of the measurement. With proper calibration, the X-ray absorption technique can determine the absolute mass and the mass distribution using equation (1). Owing to the complexity of the fuel composition, μ_M could not be obtained accurately by calculation. The absorption coefficient was measured in a sample cell of known geometry to be $\mu_M = 131$ mg^{-1}. The uncertainty of the calibration process was determined by successive trials to be ~1.5%. This reflects the systematic uncertainty of the mass calibration. We also measured the anomalous absorption above and below the Ce L_{III} edge at 5.723 keV to confirm this calibration.

3. Results and discussion

Plots of the time-dependent X-ray transmission measured on the central spray axis at distances of 1 mm and 4 mm from the nozzle are shown in Fig. 2. The linearity of the APD response (output pulse voltage) was proportional to the beam intensity within each synchrotron pulse over the range used in our experiment, and is shown in the inset to Fig. 2. The origin of the time axis of Fig. 2 is set to about 0.1 ms before the spray event. This plot shows features that we found to be typical of our measurements along the spray axis. For the data measured 1 mm from the nozzle, before the spray intersects the measurement point ($t < 0.1$ ms), the X-ray transmission is near unity. This region of the plot serves as our determination of the baseline transmission. At a later time ($t = 0.11$ ms) the fuel intersects the X-ray beam, and a sharp decrease appears in the transmission. This leading edge of the fuel spray appears very abruptly, indicating a very distinct boundary between ambient gas and fuel spray. Behind the abrupt leading edge is a large sharp spike in the transmission data as the spray travels farther from the nozzle. The leading edge represents a minimum in the transmission, the highest-density region of the entire spray. After this high-density region, the transmission increases and oscillates over a range of a few percent transmission. At an even later time ($t = 0.5$ ms), the trailing edge appears as the fuel exits the X-ray beam and the transmission returns to near the baseline value. The trailing edge of the transmission curve is also distinct though not as abrupt as the leading edge, an indication that the trailing edge of the spray is not as sharp. Note that the transmission is greater than unity after the injection because the vaporization of the fuel displaces the strongly attenuating SF_6 gas, an effect that reverses when using N_2 in the injection chamber.

Fill gas

Avalanche photodiode

Ion chamber

Ion chamber

6 keV X-ray beam

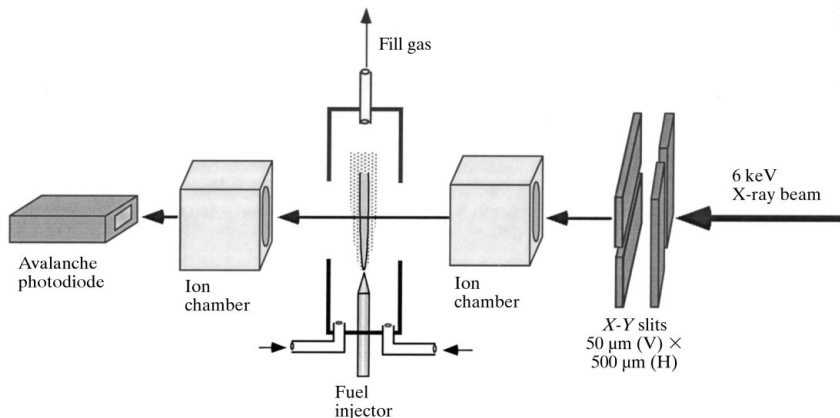X-Y slits 50 µm (V) $\times$ 500 µm (H)

Fuel injector

Figure 1
Schematic of experimental setup.

Based on the transmission values and the mass calibration procedure, one can evaluate the amount of the test fuel quantitatively. Thus, the ordinate of Fig. 2 can be transformed to mass of fuel in the X-ray beam according to equation (1), which results in a time-resolved mass measurement for each point at which the transmission was measured.

The measurements made in this work were line-of-sight measurements, and the masses measured are integrated over the breadth of the entire spray. The mass measurements alone are not sensitive to the state of the fuel and cannot distinguish between liquid, droplets or vapor. However, with an appropriate model of the spray plume, the line-of-sight mass measurements can be used to calculate the fuel volume fraction, an important spray parameter that has never been quantitatively measured. The details of these calculations are described below.

Fig. 3 shows the measured radial distribution of the fuel mass for distances of 1, 4 and 6 mm from the nozzle. The curves are Gaussian functions that have been adjusted to fit the measured data. Since the radial distributions are reproduced well by a Gaussian function, modeling the radial distribution of the fuel

density as a Gaussian function along the radial axis is reasonable. If we assume that the mass distribution is circularly symmetric (an assumption that is supported by the symmetry above and below the axis, and by the fact that we are using a circular nozzle), the mass of the fuel $M(y,t)$ in the beam at one instant, t, can be expressed as

$$M(y,t) = M_0(t)\exp\left(-y^2/2a_t^2\right), \tag{2}$$

where M_0 and a_t are the peak value and the width of the Gaussian, respectively, and y is the radial coordinate of the position. A least-squares fitting procedure was used to adjust the parameters M_0 and a_t of equation (2) to fit the mass distributions in Fig. 3. These parameters are then used to calculate the radial fuel density distribution, $c(r,t)$,

$$c(r,t) = M(r,t)/\left[A(2\pi)^{1/2}a_t\right], \tag{3}$$

where r is the distance from the spray axis in the plane perpendicular to that axis and A is the cross-sectional area of the X-ray beam. The statistical uncertainty of the density calculation was estimated to be less than 5% for the region within 6 mm of the
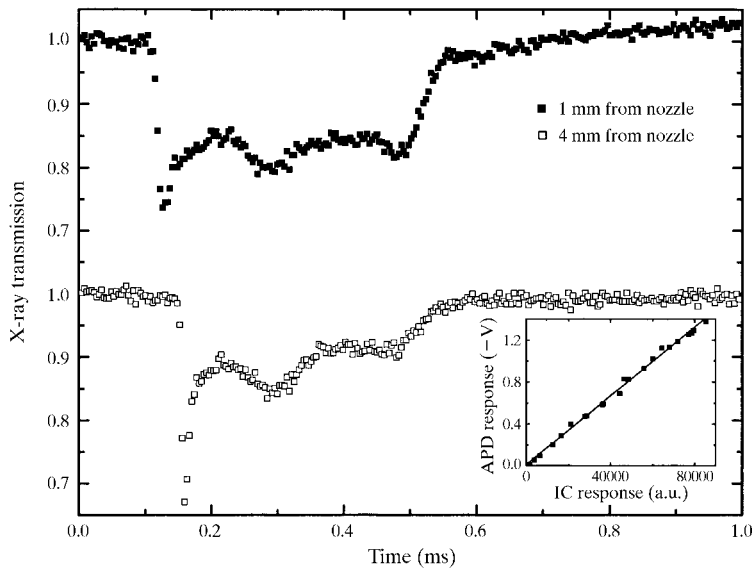

Figure 2
Time evolution of the X-ray transmission on the spray axis at 1 mm and 4 mm from the nozzle. The inset shows the linear relationship between the APD response and the ionization chamber (IC) response over the intensity range of the absorption measurement.
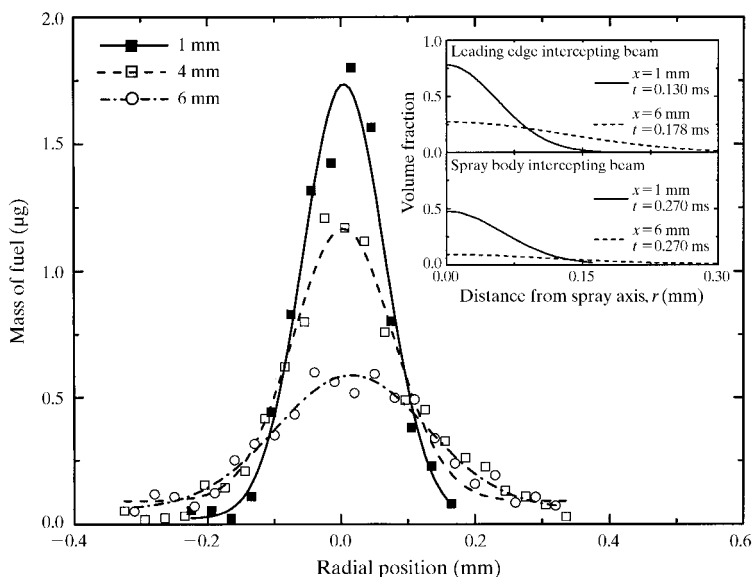

Figure 3
Measured fuel mass as a function of the radial position at three different axial positions. In this figure, the fuel mass was measured in the main body of the spray at time t = 0.27 ms. The curves are Gaussian fits to the data. The inset shows the calculated volume fraction at distances of 1 and 6 mm for the leading edge (upper panel) and main body (lower panel) of the spray. A volume fraction equal to unity implies the density of pure liquid fuel. The data shown were measured at 500 bar injection pressure and 300 µs injection duration using SF_6 as the chamber gas.

nozzle. The volume fraction is then obtained by dividing the density by the pure liquid density.

The fuel volume fraction is plotted in the inset to Fig. 3 for the leading edge of the spray (upper panel) and the main body of the spray (lower panel) at distances, x, of 1 and 6 mm from the nozzle. The most striking feature of these plots is that the density of the fuel spray was significantly less than that of the bulk liquid fuel, even as close as 1 mm from the nozzle. The only part of the spray with a density close to the bulk liquid density was the very thin leading edge of the spray, which had a maximum density of about 75% of that of the liquid at a distance of 1 mm from the nozzle. By the time this thin leading edge had traveled 6 mm from the nozzle, the volume fraction had dropped to about 25%. The main body of the spray, the region that has been termed the 'liquid core', is actually composed of a liquid/gas mixture. At a distance of 1 mm from the nozzle, the spray core had a maximum volume fraction of less than 50%. At 6 mm from the nozzle, the volume fraction of the spray core had dropped to less than 10%. Clearly, the large pressure gradient generated by the injector was sufficient to partially atomize the fuel as it left the nozzle under these conditions. Even as close as 1 mm from the nozzle, the spray did not contain an intact liquid core. We have observed similar results with other injection pressures, durations and fill gases.

As indicated in Fig. 2, the fast temporal resolution of the measurement ensured that the leading and trailing edges of the spray were precisely determined. The relationship between the time the spray arrived or left the X-ray beam and the axial location of the beam provided a way to evaluate the axial component of the velocity of the leading and trailing edges. Because the spray divergence angle is small (less than 5° as determined by this work), the radial component can be neglected, and the axial component can be regarded as the spray speed. In Fig. 4, the axial distance is plotted *versus* the arrival time of the leading edge and the departure time of the trailing edge. Also shown are polynomial fits to the leading and trailing edge penetration data. The derivatives of these curves are a measurement of the speed of the spray and are plotted in the inset of Fig. 4. The leading edge speed near the nozzle was $\sim$50 m s^{-1} and increased until a distance of $\sim$15 mm, when it reached a steady value of $\sim$157 m s^{-1}. This speed is slightly higher than the speed of sound in pure SF$_6$ gas ($\sim$140 m s^{-1}). The trailing edge speed (>500 m s^{-1} for $x < 5$ mm)

is much higher than that of the leading edge and quickly decreases over the entire measurement range. To our knowledge, this is the first measurement of the speed of the trailing edge of a high-pressure fuel spray, which is not accessible to optical techniques because of the high droplet density in the spray core.

There are several implications of the higher velocity of the trailing edge of the spray. The leading edge velocity is limited by the sonic pressure of the ambient gas. However, the bulk of the spray can travel faster than the leading edge, resulting in compression of the region near the leading edge. This compression accounts for the high density ($\sim$70% of the bulk liquid density) in the very thin leading edge, the most dense region of the spray. It demonstrates that the spray is compressible, another indication that the bulk of the spray did not consist of a pure liquid, even very close to the nozzle.

It is important to note that in this work we can only measure the speed at the leading and trailing edges of the spray – the speed of the bulk cannot be readily determined. Because the spray is compressible, different regions can travel at different speeds. However, we speculate that the bulk travels at a speed similar to that of the trailing edge, with only the leading edge slowed by the impact with the ambient gas. When the fuel travels faster than the speed of sound, shock waves might be generated in the injection chamber. Currently, we are searching for more direct evidence to demonstrate the existence of such shock waves.

4. Summary

We have described the use of monochromatic X-ray radiography to study supersonic diesel fuel sprays in a highly quantitative and highly time-resolved manner. The preliminary results indicate that the core region near the nozzle is composed of a liquid/gas mixture with a density less than 50% of the bulk liquid density as close as 1 mm from the nozzle (500 bar, 300 μs, SF$_6$ gas). In addition, the supersonic nature of the sprays generated by this type of injection system has been demonstrated by the experiments. The success of the measurements has demonstrated that the X-ray technique is well suited for elucidating the spray structure near the nozzle orifice. The information obtained should stimulate theoretical simulation of spray processes in this region
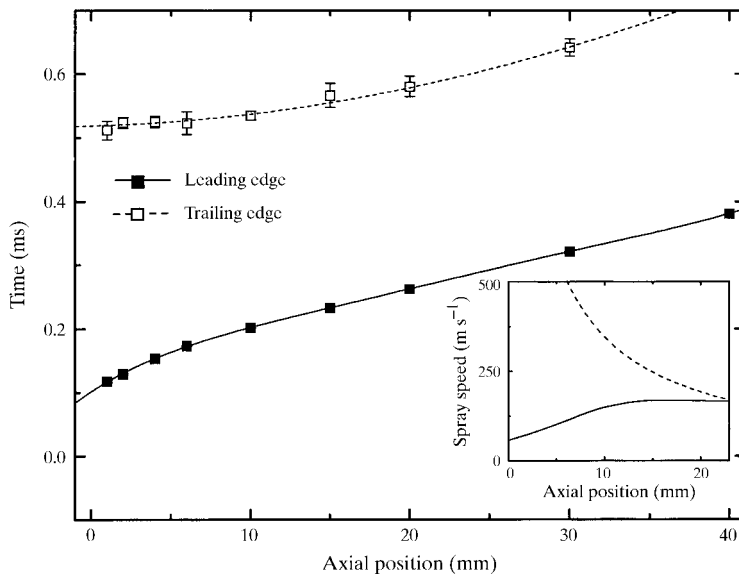

Figure 4
Penetration of the leading and trailing edges of the spray. The curves are polynomial fits to the penetration data. The inset shows the speed of the leading and trailing edges of the spray determined by differentiation of these polynomials.

and establish a knowledge base of spray breakup mechanisms and droplet interactions, which are key to realistic combustion modeling and the design of injection systems. The time-resolved monochromatic X-ray radiographic technique will likely find applications not only in the various fields of spray technology but also in other research and development areas dealing with highly transient and optically impenetrable structures, such as aerosols and dense plasmas of high-Z materials. We note that the point-by-point technique currently used in this study is inefficient, and the development of fast position-sensitive X-ray detectors is essential to improve the efficiency of the measurement (Rossi *et al.*, 1999). We also speculate that other X-ray techniques, such as fluorescence and small-angle scattering, may also be useful for the investigation of other aspects of fuel spray structure.

References

Adrian, R. J. (1991). *Annu. Rev. Fluid Mech.* **23**, 261–301.

Chen, G., Mazumder, M. M., Chang, R. K., Swindal, J. C. & Acker, W. P. (1996). *Prog. Energy Combust. Sci.* **22**, 163–188.

Coil, M. A. & Farrell, P. V. (1995). *Soc. Automot. Eng.* SAE 950458.

Henke, B. L., Gullikson, E. M. & Davis, J. C. (1993). *Atom. Data Nucl. Data Tables*, **54**, 181–342.

Hiroyasu, H. (1991). *Fifth International Conference on Liquid Atomization and Spray Systems*, Gaithersburg, 17–31 July 1991. Gaithersburg, MD: National Institute of Standards and Technology.

Lang, J. C., Srajer, G., Wang, J. & Lee, P. L. (1999). *Rev. Sci. Instrum.* **70**, 4457–4462.

Long, W.-Q., Ohtsuka, H. & Obokata, T. (1996). *JSME Intl*, **39**, 554–561.

Maly, R. R., Mayer, G. W., Reck, B. & Schaudt, R. A. (1991). *Soc. Automot. Eng.* SAE 910727.

Rossi, G., Renzi, M., Eikenberry, E. F., Tate, M. W., Bilderback, D., Fontes, E., Wixted, R., Barna, S. & Gruner, S. (1999). *J. Synchrotron Rad.* **6**, 1096–1105.

Shimizu, I., Shimoda, M., Suzuki, T. & Emori, Y. (1982). *Soc. Automot. Eng.* SAE 820355.

Woodward, R. D., Pal, S., Santoro, R. J. & Kuo, K. K. (1995). *Recent Advances in Spray Combustion: Spray Atomization and Drop Burning Phenomena*, pp. 185–210. Reston, VA: American Institute of Aeronautics and Astronautics.

Yeh, C. N., Kamimoto, T., Kobori, S. & Kosaka, H. (1993). *Soc. Automot. Eng.* SAE 932652.